

Clicked bis-PEG-Peptide Conjugates for Studying Calmodulin-Kv7.2 Channel Binding

M. Angeles Bonache,^a Alessandro Alaimo,^b Covadonga Malo,^b Oscar Millet,^c Alvaro Villarroel,^b Rosario González-Muñiz^{a,*}

^aInstituto de Química-Médica (IQM-CSIC), Juan de la Cierva 3, 28006 Madrid, Spain.

^bUnidad de Biofísica, CSIC-UPV/EHU, Universidad de País Vasco, Barrio Sarriena s/n, 48940 Leioa, Spain.

^cStructural Biology Unit, CICbioGUNE, Bizkaia Technology Park, 48160 Derio, Spain

ABSTRACT: The recombinant Kv7.2 calmodulin (CaM) binding site (Q2AB CaMBD) shows a high tendency to aggregate, thus complicating biochemical and structural studies. To facilitate these studies we have conceived bis-PEG-peptide CaMBD-mimetics linking helices A and B in single, easy to handle molecules. Short PEG chains were selected as spacers between the two peptide molecules, and a Cu(I)-catalyzed cycloaddition (CuAAC) protocol was used to assemble the final bis-PEG-peptide conjugate, through the convenient functionalization of PEG arms with azide and alkyne groups. The resulting conjugates, with a certain helical character in TFE solutions (CD), showed nanomolar affinity in a fluorescence CaM binding *in vitro* assay, higher than just the sum of the precursor PEG-peptides affinities, thus validating our design. The approach to these first described examples of Kv7.2 CaMBD-mimetics could pave the way to chimeric conjugates merging helices A and B from different Kv7 subunits.

Key words: PEG-peptide conjugates, Click chemistry, Calmodulin binding, Ion Channels, Fluorescence.

INTRODUCTION

Kv7.2 and Kv7.3 subunits, encoded by the KCNQ2 and KCNQ3 genes, are the main components of the M-current, a voltage-dependent, non-inactivating K^+ current that plays a critical role in controlling the activity of both peripheral and central neurons.¹

Like all Kv channels, the α subunits of the five members of the KCNQ family share a common core structure of six transmembrane segments with a voltage sensing domain (S1–S4) and a pore domain (S5 and S6; see Figure 1).² The large intracellular C-terminal tail contains four helical regions (A–D) crucial to channel assembly, gating and regulation, including the intercommunication with different regulatory factors. Discontinuous segments A and B, with high probability of adopting α -helix conformations, constitute the binding site for calmodulin (CaM),³ a ubiquitous calcium sensor which mediates traffic to the plasma membrane and Ca^{2+} -dependent inhibition of Kv7 channels.⁴⁻⁶ Some spontaneous mutations located in helix A or B interfering with CaM binding, are linked to familial Benign Familial Neonatal Convulsions (BFNC),¹ a dominantly inherited idiopathic human epilepsy. The “Benign” tag is misleading, because these mutations are often associated with poor outcomes.^{7, 8}

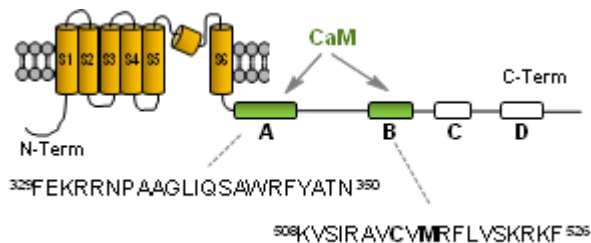


Figure 1. Topological representation of a Kv7.2 subunit and its calmodulin binding sites. Below are the partial sequences of helix A and B used in this paper.

Although the knowledge about the Kv7-CaM interrelationship has advanced in recent years,⁹⁻¹¹ fundamental aspects of the interaction are not known. Thus, a recent X-ray structure of the complex between CaM and the Kv7.4 helix B peptide has trapped Ca^{2+} /CaM wrapping around the helix B in an antiparallel 1-14 binding-mode.¹² However, this study only provides partial information about CaM binding to the Kv7 channels, since these channels have two CaM binding sites that are essential for the final binding mode of the complex.^{3, 13} For instance, it is expected that helices A and B interact with each other while binding to CaM,¹⁴ as described for other channels.¹⁵ In fact, we have found that CaM binds to either recombinant or synthetic helix A or B peptides, and the two sites cooperate to increase the affinity for this Ca^{2+} sensor.¹⁴ However, the long loop of 141 residues between helices A and B does

not seem to be directly involved in the interaction with CaM,³ although this linker regulates both surface expression and protein production.¹⁶

The remarkable tendency of the recombinantly produced Kv7.2 CaM binding site (Q2AB CaMBD) to aggregate has precluded detailed biochemical and structural studies, and the chemical synthesis of the Q2AB CaMBD (> 100 amino acids) is impractical. An alternative to overcome these technical obstacles is to synthesize Q2AB CaMBD-mimetics that retain the fundamental properties regarding CaM-binding by joining A and B fragments in a unique molecule.

Herein, we report the design and synthesis of two polyethyleneglycol PEG-peptide conjugates combining the amino acid sequence of helices A and B of Kv7.2. A 1,4-disubstituted 1,2,3-triazolyl scaffold was selected to join the two helical peptides in a single molecule (Figure 2). This heterocycle is easily accessible from alkyne and azide-substituted precursors using click chemistry, a well-recognized, powerful tool in bioconjugation.¹⁷ As a first requirement for these conjugates to be further used as biological probes, we also report that the binding properties recapitulate those of the recombinant Q2AB CaMBD, and are not the result of the sum of the values of its precursors.

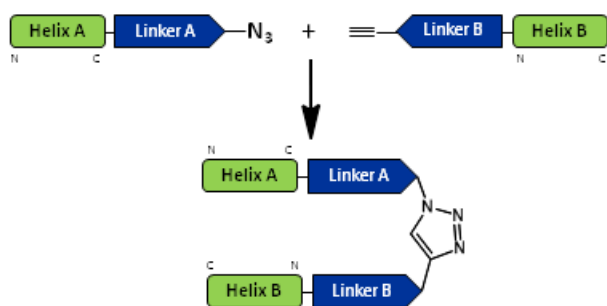


Figure 2. Schematic representation of clicked peptide-conjugates derived from the amino acid sequence of Kv7.2. Linker: short PEG chains.

RESULTS AND DISCUSSION

Design of PEG-peptide conjugates. Peptides Ac-³²⁹FEKRRNPAAGLIQSAWRFYATN³⁵⁰-NH₂ (derived from Kv7.2 helix A) and Ac-⁵⁰⁸KVSIRAVCVMRFLVSKRKF⁵²⁶-NH₂ (a fragment of Kv7.2 helix B) were selected based on the principles of consensus sequence reported.^{14, 18} A two point-mutation peptide Ac-⁵⁰⁸KVSIRAVRVLRLFLVSKRKF⁵²⁶-NH₂, in which the native Cys⁵¹⁵ and Met⁵¹⁷ residues of Kv7.2 are changed to Arg and Leu (as in Kv7.3 and Kv7.4), respectively, was also contemplated by technical reasons (see below). We hypothesized that the A and B helices adopt an antiparallel disposition upon CaM binding, as described in the structure of the related SK channel CaMBD/Ca²⁺/CaM complex,¹⁵ and consequently the linkers to connect both molecules were incorporated at C- and N-terminal

positions, respectively (Figure 2). For this purpose, C-terminal Asn and N-terminal Lys functionalized side-chains were considered appropriate points for anchoring the spacer.

Taking into account that solubility could be an issue for peptides longer than 6 residues, the linker could be selected to improve this property in the bis-A-B peptide conjugates in aqueous media. To this end, we envisaged the use of short polyethyleneglycol (PEG) units, a well-established strategy for peptide modification that improves not only aqueous solubility, but also increases enzymatic stability and could reduce antigenicity and immunogenicity.¹⁹⁻²¹ Moreover, site-specific PEGylation of peptides was described to contribute to the stabilization of particular peptide secondary structures.²²⁻²⁴ To connect the PEG-peptides we opted for a 1,4-disubstituted 1,2,3-triazolyl ring, which could be built by Cu(I)-catalyzed azide-alkyne cycloaddition, one of the most widely used Click chemistry reactions.¹⁷ This reaction is highly chemoselective, and can be performed in aqueous solution under mild conditions, being compatible with deprotected peptide side-chain functional groups.²⁵⁻²⁷ In fact, this 1,3-dipolar cycloaddition was already successfully applied to combine peptides and PEG-containing molecules, as in the synthesis of biodegradable peptide-based hydrogels and in the fluorescent labeling of nisin lantibiotics, to cite two representative examples.^{28, 29}

To provide the conjugate molecule with certain flexibility upon CaM binding, a commercial 1-aminotriethyleneglycol derivative, bearing an azido group at the end, was chosen to get the functionalize Asn³⁵⁰ residue of helix A (Figure 3). For helix B-derived peptides, a pent-4-ynoyl-substituted 1-aminodiethyleneglycol-7-carboxyl moiety was attached in two steps to the Lys⁵⁰⁸ amino side-chain group. This led to final linkers of similar length on both peptides that, upon transformation into the triazole-PEG-peptide conjugates, could force the motion of the two peptide arms in an antiparallel disposition. As the triazole ring can constitute a bend point, we preferred the indicated side-chain to side-chain location over placing it at the very N- or C-terminal positions, which could result in conjugates unable to bring close together the two peptides or that could align them in a wrong way.

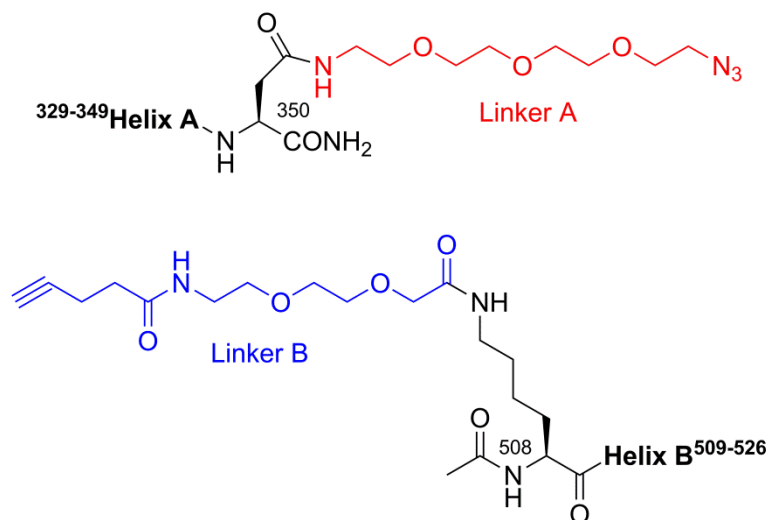
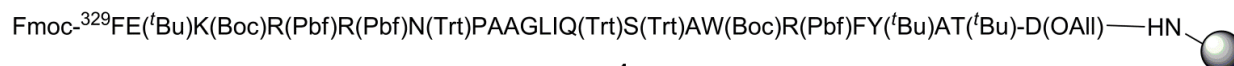
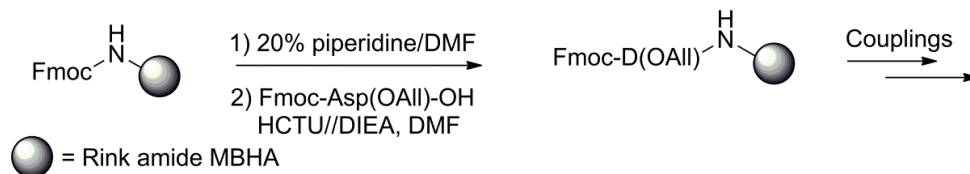


Figure 3. Polyethyleneglycol linkers selected for the conjugation of peptides derived from Kv7.2 helices A and B sequences

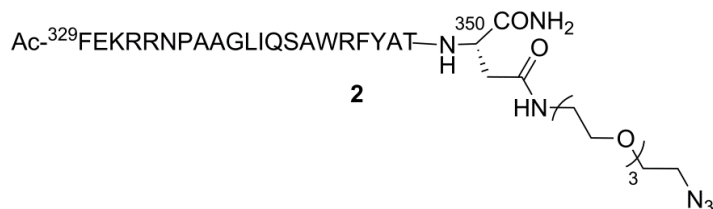
Synthesis. The synthesis of single peptide derivatives, Helix A³²⁹⁻³⁵⁰-PEG-azide (**2**), Alkyne-PEG-Helix B⁵⁰⁸⁻⁵²⁶ (**5**) and its double mutant **6**, were performed in parallel, following solid-phase protocols (Schemes 1 and 2). A low load Rink amide MBHA polystyrene resin (0.34 mmol g⁻¹) was used to prevent aggregation problems. Protecting groups are those normally used in an Fmoc/^tBu strategy, and peptides were elongated on the resin using HCTU as coupling agent. All compounds were isolated in high purity as C-terminal amides and acetylated at the N-terminal amino group. To allow the on-resin regioselective functionalization of peptides, an Fmoc-Asp(OAll)-OH was incorporated as the first amino acid during the synthesis of resin bound peptide **1** (Scheme 1), while an Fmoc-Lys(Alloc)-OH was introduced as the last residue in the sequence elongation to protected peptides **3** and **4** (Scheme 2). These All and Alloc groups can be orthogonally deprotected to facilitate the site-specific PEGylation at the Asp³⁵⁰ and Lys⁵⁰⁸ side-chains.^{30, 31}

Thus, after elongation to resin bound peptide **1**, the Fmoc group was removed, the N-terminal NH₂ was acetylated, followed by the Pd-catalyzed deallylation of the C-terminal Asp residue side-chain. On resin coupling with a DMF solution of 11-azido-3,6,9-trioxaundecen-1-amine in the presence of HCTU afforded the corresponding Asn derivative, which upon acidic treatment led to cleavage from the resin, and concomitant side chain deprotection, to the expected Peptide-PEG-azide conjugate **2**.

Scheme 1. SPPS Synthesis of Helix A³²⁹⁻³⁵⁰-PEG-azide (2**)**



- 1**
- 20% piperidine/DMF
 - Ac₂O/DIEA
 - PhSiH₃, Pd(PPh₃)₄/ DCM
 - H₂N-(CH₂CH₂O)₃CH₂CH₂N₃, HCTU//DIEA, DMF
 - TFA-EDT-H₂O-TIS (94:2.5:2.5:1)



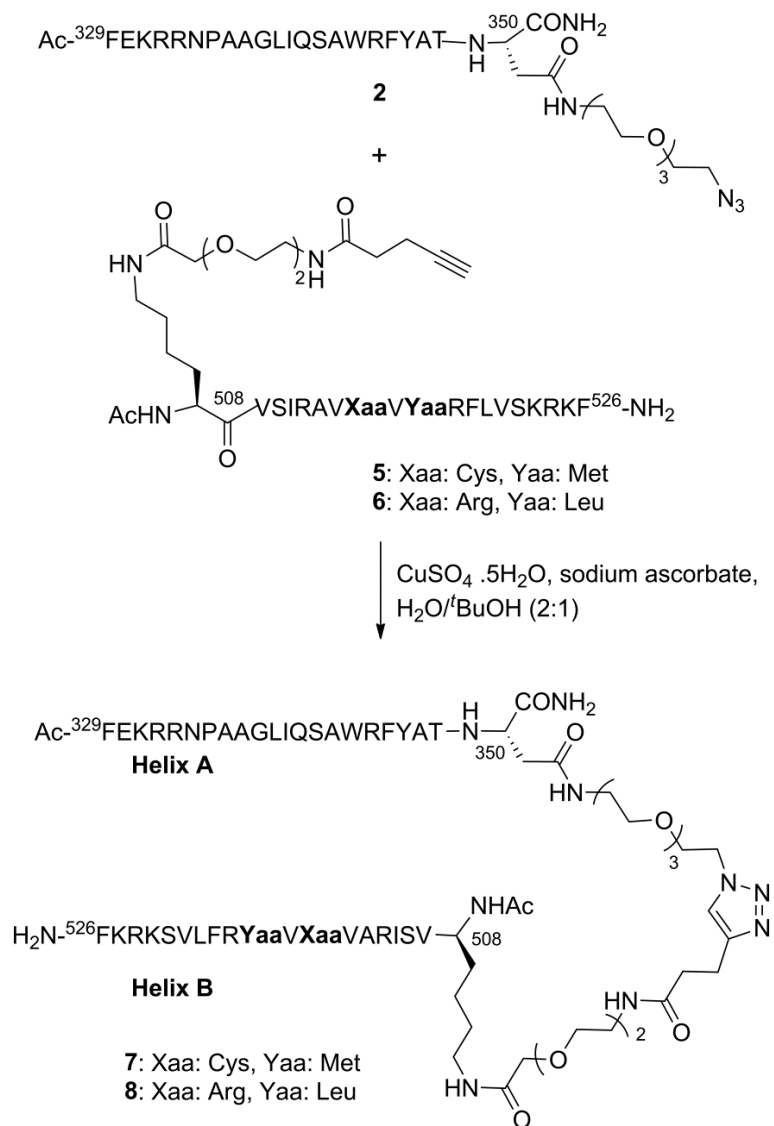
In a similar manner, resin-bound peptides **3** and **4**, after N-terminal Fmoc-deprotection and acetylation, were treated with PhSiH₃/Pd(PPh₃)₄ for Alloc group removal. Then, the free amino group of the Ac-Lys⁵⁰⁸ residue was reacted with a DMF solution of 2-[2-(Fmoc-amino)ethoxy]ethoxy]acetic acid/HCTU (Scheme 2). After the PEGylation and Fmoc removal steps, a new coupling reaction was carried out with 4-pentynoic acid/HCTU in order to incorporate the alkyne function. Finally, the obtained resins were treated with the cleavage cocktail TFA/EDT/H₂O/TIS (94:2.5: 2.5:1) to afford the unbound, deprotected Alkyne-PEG-Helix B⁵⁰⁸⁻⁵²⁶ conjugates **5** and **6**.

Scheme 2. SPPS Synthesis of alkyne-PEG-Helix B⁵⁰⁸⁻⁵²⁶

HPLC data, Figure 4) after purification of reaction crudes by reverse-phase semipreparative HPLC.

Characterization of these peptide conjugates was performed by HPLC-MS and HRMS (EI^+).

Scheme 3. Synthesis of $^{329-350}$ Helix A-PEG-triazole-PEG-Helix B $^{508-526}$ conjugates 7 and 8



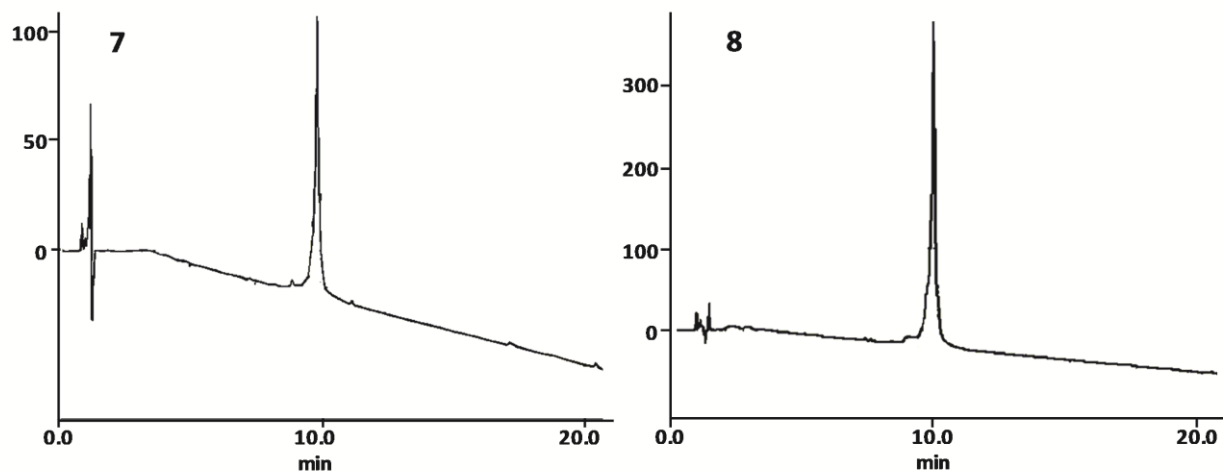


Figure 4. HPLC chromatograms of purified PEG-peptide conjugated **7** and **8** (C_{18} column, linear gradient from 5 to 80% ACN in 20 min).

CD Studies. To evaluate the ability of mono- and bis-peptide conjugates to adopt helical structures, circular dichroism (CD) were performed (Figure 5 and S2). Most peptides showed no defined structure (random coil) in aqueous solution, and only compound **7** has a certain stabilization of the helix conformation (Table 1). All of them become helical upon the addition of TFE (30%), as indicated by the characteristic double minimum at 208 and 222 nm. The fact that these peptides turn into helix conformation in the presence of the structure-inducing cosolvent could be symptomatic of a tendency to be helical in a suitable environment (i.e., in the presence of CaM). As shown in Table 1, helix B-containing conjugates **5** and **6** are highly helical (<90% helicity in TFE), while the helix character of the PEG-helix A peptide **2** is smaller (24%). Bispeptide conjugates showed an intermediate situation, with mimetic **7** being clearly more helical (35%) than analogue **8** (11%). While the C515R and M517L changes do not significantly affect helicity of PEG-peptide **6** compared to native **5**, these changes disturb in a greater extent the structuration of bis-PEG-peptide **8** related to **7**. These results suggest an interrelation between the two helical segments in the bisconjugates that is disrupted by the indicated changes.

Table 1. Experimental CD helicity (%) of peptide conjugates

Compd.	H ₂ O	30% TFE
2	2	24
5	4	94
6	3	91
7	8	33
8	1	11

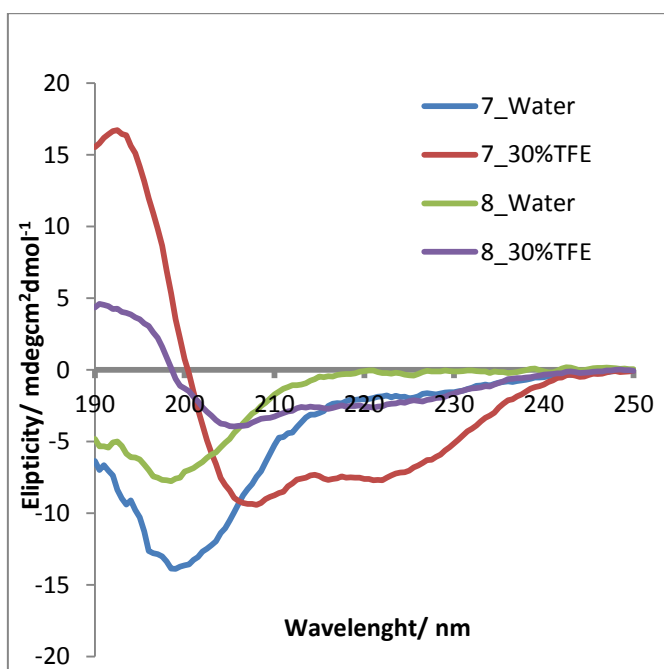


Figure 5. CD spectra of peptides **7** and **8** in H₂O and 30% TFE/H₂O at pH 5.5 and 5 °C.

CaM binding assays. To assess the ability to bind CaM, peptide conjugates ³²⁹⁻³⁵⁰Helix A-PEG-triazole-PEG-Helix B⁵⁰⁸⁻⁵²⁶ **7** and its C511R, M513L mutated analogue **8** were evaluated in a fluorescence CaM binding *in vitro* assay (emission spectra were recorded, as in Figure S3). As binding of proteins to CaM sometimes relies on the C-lobe, others in the N-lobe, or the lobe-linker or combinations of those, it is impossible to know in advance if the position of the label is going to affect binding. To avoid this issue, the experiments were performed on three differently labeled CaMs. First, titration of unspecifically dansylated CaM (D-CaM) with increasing concentrations of each peptide was carried out, both in the presence and the absence of a physiologically relevant concentration of free Ca²⁺ (Figure 6A, and S4). Then, we performed experiments on two different site-specific labeled CaMs (AEDANS-CaMs, carrying the point mutations T34C or T110C, respectively), having the AEDANS group on the CaM *N* or *C* lobe, respectively (Figure 5, B and C). Subsequently, we analyzed the data to obtain binding curves, from which binding parameters have been calculated (EC₅₀, Hill coefficient, Tables 2 and S1; K_D, Table S2).

As shown in Figure 6, bis-PEG-peptide conjugate **7** is able to augment the fluorescent emission of the reporter CaM in a saturable dose-dependent manner, indicating a direct interaction of the conjugate with CaM. The position of the reporter fluorophore had little impact of the binding affinity (Table S1), supporting the view that the obtained values are very close to the true affinity of unlabeled CaM. The affi-

ity, in the nanomolar range, is only two-fold lower than that previously determined for the recombinant A and B helices joined by the long 141 residues linker,¹⁴ and follows the same trend in the presence (lower affinity) and the absence of Ca²⁺ (higher affinity). Thus, compound **7** appears to be a reasonable mimetic for the Kv7.2 CaM binding site. Because the observed binding of bis-conjugate **7** could be explained through the interaction of CaM with a single helix (A or B) or with both helices at a time, precursors PEG-peptides **2** (helix A) and **5** (helix B) were also studied (Figure 7, and S5). In total agreement with previous results regarding recombinant or synthetic peptides derived from helix A or B,¹⁴ compound **2** (helix A) showed greater increase in fluorescence than helix B-derived compound **5**, but this latter displayed higher affinity (Tables 2 and S1). While the amplification of D-CaM fluorescent emission by PEG-peptide conjugate **2** was slightly lower than that of peptide **pA** (using the same assay), the apparent affinities were almost identical irrespective of the presence of Ca²⁺ or not. This indicates that the polyethyleneglycol has a negligible impact on binding to CaM. Compared to peptide **pB**, PEG-conjugate **5** showed decreased apparent affinities, which could be due to either a negative influence of the PEG chain or to the differences in the sequence (lack of *N*-terminal GL residues, and/or detrimental effects of the *C*-terminal KRKF sequence). Both the maximal increase in fluorescence and the apparent affinity were greater for a 1:1 mixture of compounds **2** and **5** than for each peptide conjugate alone, in concordance with previous results for an equimolar mixture **pA** and **pB**.¹⁴ While interacting with CaM, the **2+5** mixture showed a lower increase of fluorescence and apparent affinities than the covalently connected bis-conjugate **7**, suggesting a favorable role for the PEG linker in facilitating binding.

Replacement of Cys⁵¹⁵ and Met⁵¹⁷ residues of helix B in **7** by Arg and Leu, respectively, led to bis-conjugate **8**, which decreases to approximately half the fluorescence and apparent affinity (i.e doubling the EC₅₀) compared to **7** (Table 2, Figure S4). In the crystal structure of the Ca²⁺-CaM:Kv7.4 B-helix complex, this leucine was defined as a key interacting residue, occupying the main hydrophobic anchoring pocket of the Ca²⁺-N-lobe¹². As the Met by Leu change is conservative, it is expected that this Leu could contribute to the conjugate **8**-CaM interaction in the same way than in above complex. However, the more drastic replacement of Cys by Arg is suggestive of an important role of Cys⁵¹⁵ in the binding of Kv7.2 to CaM. The decreased helical stability of compound **8** in solution could also be related, at least in part, to the diminished affinity, requiring of higher energy to accommodate within the CaM-peptide complex.

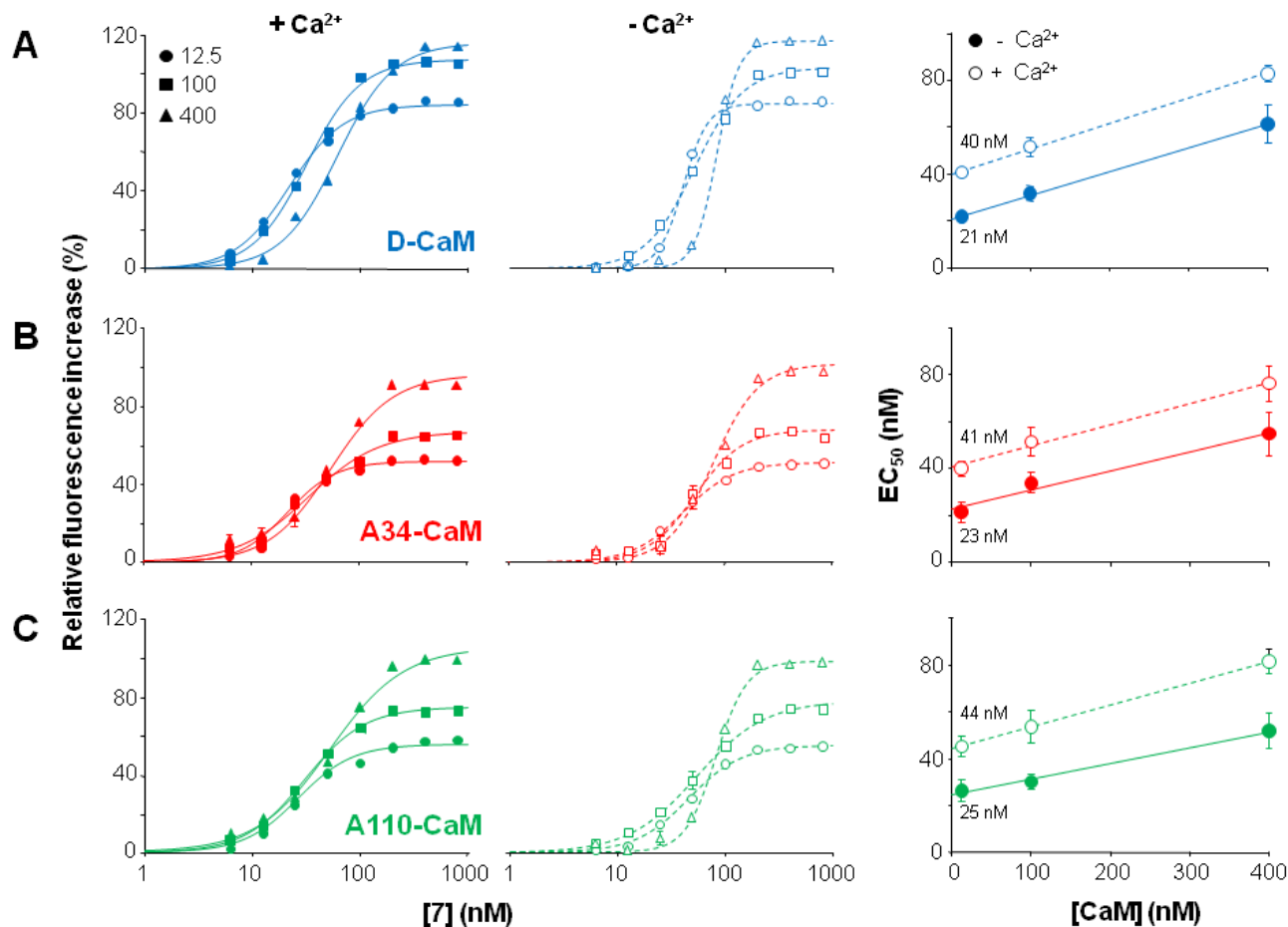


Figure 6. Dose-response interaction of peptide 7 (A-B) with fluorescently labeled CaMs. The symbols indicate the total concentration of tagged-CaM used in each series. **A)** Relative concentration-dependent enhancement of D-CaM fluorescence (blue) in the absence (left, filled symbols) and presence (middle, open symbols) of $3.9 \mu\text{M}$ free Ca^{2+} . Right, extrapolation to the true affinity. Apparent dissociation constants (EC_{50}) for the 7/CaM complex are shown as a function of the [CaM]. **B)** and **C)** Similar characterization using A34-CaM (red) or A110-CaM (green), respectively. Data represent the means \pm S.E.M. from three or more independent experiments at each concentration of fluorescent labeled-CaM. The error bars are smaller than the symbols. The parameters used to fit a Hill equation to the data, using 12.5 nM fluorescent CaM, can be found in Table 2 and S1. The K_d values can be found in Table S2.

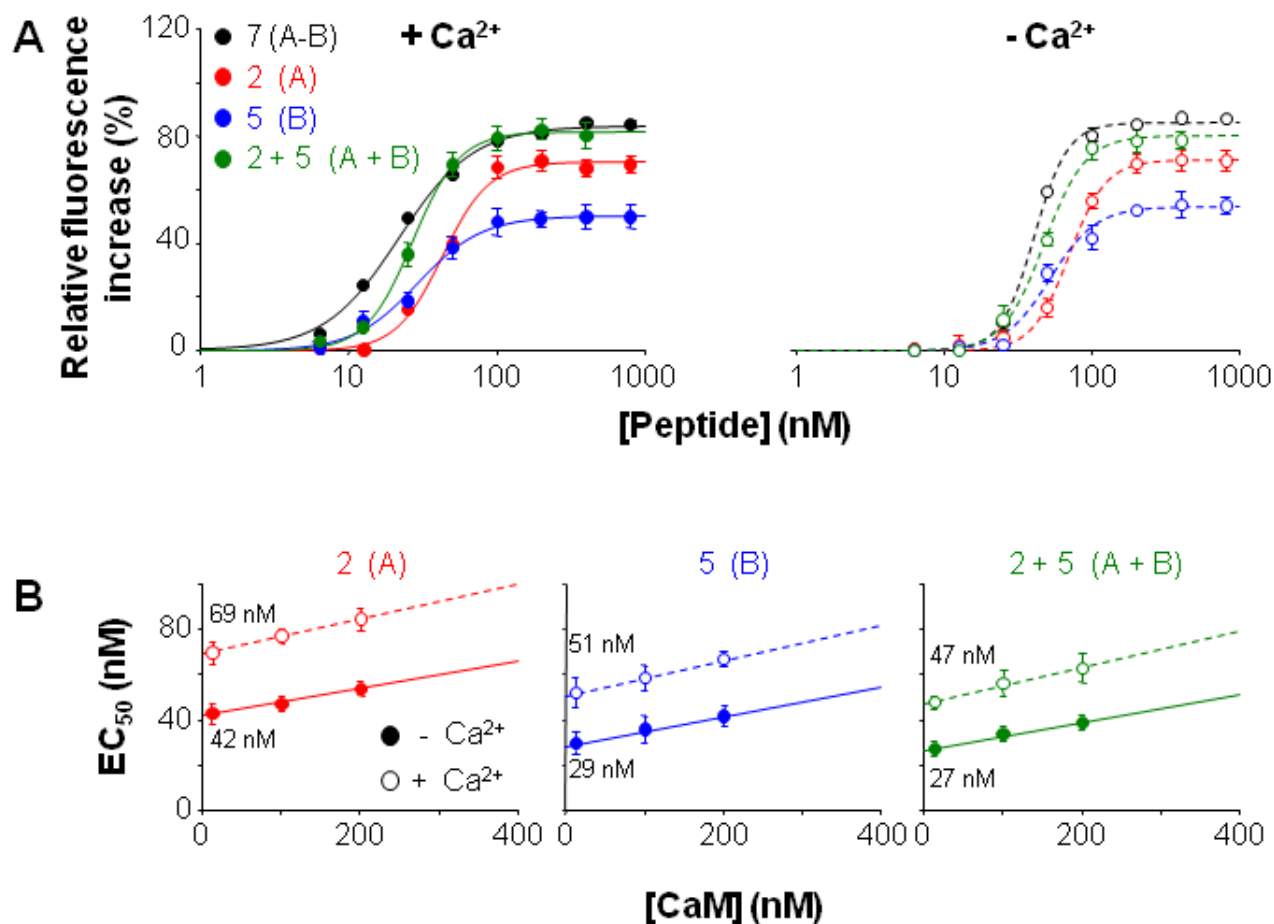


Figure 7. The binding mode to peptide 7 is not the result of a linear interaction with its constituent peptides 2 and 5. A) Titration of 12.5 nM D-CaM fluorescence with peptide 2 (red), peptide 5 (blue) and an equimolar mixture of both (2 + 5, green). The black lines are the best fits to the data obtained for peptide 7. The experiments were performed in the absence (left, filled symbols) and presence (right, open symbols) of 3.9 μM free Ca^{2+} . Data represent the means \pm S.E.M. from three or more separate experiments performed at each concentration of D-CaM. The error bars are smaller than the symbols. **B)** EC_{50} values obtained from binding curves were plotted versus [D-CaM] in order to extrapolate to the true affinities (K_d). The parameters used to fit a Hill equation to the data, using 12.5 nM fluorescent CaM, can be found in Table 2 and S1. The K_d values can be found in Table S2.

Table 2. Summary of the binding parameters obtained using 12.5 nM D-CaM.

Peptide	- Ca ²⁺ (EGTA 10 mM)			+ Ca ²⁺ (3.9 μM)		
	Maximal fluo- resc. increase	EC ₅₀ (nM)	h (n)	Maximal fluo- resc. increase	EC ₅₀ (nM)	h (n)
7 (A-B)	84.3 ± 1.3	21.7 ± 1.1	1.7 ± 0.1 (4)	85.6 ± 0.7	40.5 ± 0.7	3.8 ± 0.2 (4)
2 (A)	70.7 ± 1.6	42.7 ± 2.2	2.7 ± 0.3(4)	71.4 ± 1.2	69.8 ± 2.3	3.4 ± 0.2 (4)
5 (B)	50.6 ± 1.2	29.1 ± 2.1	1.9 ± 0.3 (4)	53.4 ± 1.7	51.8 ± 3.7	2.8 ± 0.5 (4)
2 + 5	81.8 ± 0.8	26.9 ± 0.7	2.7 ± 0.1 (4)	80.1 ± 1.5	47.3 ± 1.6	3.1 ± 0.3 (4)
8 (A-B Mut)	44.6 ± 1.5	48.6 ± 3.6	2.7 ± 0.4 (3)	46.1 ± 0.7	88.6 ± 3.5	3.1 ± 0.3 (3)
Q2AB ^{a,b}	111 ± 1.4	11.0 ± 0.5	1.6 ± 0.3	115 ± 2.1	27.1 ± 1.2	3.4 ± 0.5
pA ^{a,c}	75 ± 3.9	42.9 ± 0.6	2.7 ± 0.6	96 ± 7.1	68.7 ± 9.7	1.7 ± 0.3
pB ^{a,d}	35 ± 1.3	18.6 ± 1.8	2.0 ± 0.3	54 ± 1.5	43.1 ± 2.3	2.7 ± 0.3

^a Data from reference 14, using the same assay. ^b Q2AB (recombinant protein, Gly³¹⁰-Leu⁵⁴⁸ region Kv7.2). ^c pA: ³²⁹FEKRRNPAAGLIQSAWRFYAT³⁴⁹. ^d pB: ⁵⁰⁴GLKVSIRAVCVMRFLVS⁵²².

CONCLUSIONS

We have designed and synthesized a bis-PEG-peptide conjugate, HelixA³²⁹⁻³⁵⁰-PEG-triazole-PEG-HelixB⁵⁰⁸⁻⁵²⁶ (**7**), which merges in a molecule the Kv7.2 helices A and B, implicated in the intercommunication with CaM. After SPPS of the corresponding azide-PEG- and alkyne-PEG-precursor peptides, both helices were combined through 1,2,3-triazole click chemistry. CaMBD-mimetic **7**, composed of 42 amino acid residues in total, is able to bind to CaM with high affinity, only two fold lower than that a recombinant protein containing both helices (239 residues). The affinity was virtually the same in spite of the fluorophore position in CaM, suggesting that the values obtained can be extrapolated to the true affinity for unlabeled CaM. This conjugate could be a useful biological probe to further investigate the association between CaM and Kv7.2 channel, and to better understand its regulation by Ca²⁺. Mutation of a couple of residues in helix B reduces the helical character of the bisconjugate and points to an important role of Cys⁵¹⁵ residue in the binding of Kv7.2 to CaM. Finally, the synthetic approach described here could have application for the preparation of chimera conjugates, combining helices A and B from different Kv7 subunits, or, in a more general sense, for target sites conformed by dispersed segments within a protein.

EXPERIMENTAL PROCEDURES

Materials. All reagents were of commercial quality. O-(6-Chlorobenzotriazol-1-yl)-*N,N,N',N'*-tetramethyluroniumhexafluorophosphate (HCTU), *N,N*-diisopropylethylamine (DIEA), 11-azido,3,6,9-trioxaundecen-1-amine, 2-[2-(Fmoc-amino)ethoxy] ethoxy]acetic acid, 4-pentynoic acid, $\text{CuSO}_4 \cdot 5\text{H}_2\text{O}$, sodium ascorbate, tetrakis(triphenylphosphine)palladium [$\text{Pd}(\text{PPh}_3)_4$], phenylsilane (PhSiH_3), trifluoroacetic acid (TFA), 1,2-ethanedithiol (EDT) and triisopropylsilane (TIPS), by SIGMA-ALDRICH. Anhydride acetic (Ac_2O) by Scharlau. *N*-Fluorenyl-9-methoxycarbonyl (Fmoc) protected L-amino acids (Fmoc-Thr(*t*Bu)-OH, Fmoc-Ala-OH, Fmoc-Tyr(*t*Bu)-OH, Fmoc-Phe-OH, Fmoc-Arg(Pbf)-OH, Fmoc-Trp(Boc)-OH, Fmoc-Ser(Trt)-OH, Fmoc-Gln(Trt)-OH, Fmoc-Ile-OH, Fmoc-Leu-OH, Fmoc-Gly-OH, Fmoc-Pro-OH, Fmoc-Asn(Trt)-OH, Fmoc-Lys(Boc)-OH, Fmoc-Glu(*t*Bu)-OH, Fmoc-Met-OH, Fmoc-Cys(Trt)-OH, Fmoc-Lys(Alloc)-OH, Fmoc-Asp(OAll)-OH) and Rink amide MBHA resin LL (100-200 mesh, loading 0.34 mmol/g) were provided by NOVABIOCHEM. *N,N*-dimethylformamide (DMF) and dichloromethane (DCM) were dried and purified by standard methods.

General SPPS procedures for the synthesis of PEG-peptide conjugates.

Coupling procedure. Rink amide MBHA resin (500 mg, 0.17 mmol) previously swollen in DMF and DCM (1ml/100mg of resin, 30 s x 4), was treated with 20% piperidine in DMF (1 x 5min) and (1 x 20 min) and washed with DMF/DCM/DMF/DCM/DMF (4 x 0.5 min). In each coupling step, the appropriate Fmoc amino acid (0.34 mmol, 2 equiv.) was treated with HCTU/DIEA (0.34 mmol, 2 equiv.) in dry DMF (1mL/100mg of resin) at room temperature for 1 h. The coupling efficiency was monitored by the ninhydrin test and, when necessary, repeated with a fresh portion of Fmoc-amino acid and the indicated coupling reagents.

Acetylation method. The Fmoc-resin-bounded peptide, previously swollen, was treated with 20% piperidine in DMF (1 x 5 min) and (1 x 20 min) and washed with DMF/DCM/DMF/DCM/DMF (4 x 0.5 min). Acetylation reactions were performed with DIEA (3.4 mmol) and Ac_2O (3.4 mmol) in DMF for 1 h and washed with DMF/DCM/DMF/DCM/DMF (4 x 0.5 min).

Removal of Alloc and Allyl protecting groups. The resin bounded, fully protected peptide, previously swollen, was purged with Ar and treated with a solution of $\text{Pd}(\text{PPh}_3)_4$ (20 mg, 0.015 mmol) and PhSiH_3 (0.5 ml, 3.6 mmol) in anhydrous DCM (1 ml/100 mg of resin). The reaction mixture was stirred for 45 min. This procedure was repeated once more time. The resin was washed with DCM/DMF/ $\text{Et}_2\text{NCS}_2\text{Na}$ (0.02M)/DMF/DCM (4 x 0.5 min).

Cleavage step. Cleavage of peptides from the resin, and concomitant deprotection of side-chains, was performed using TFA/EDT/ H_2O /TIPS (94:2.5:2.5:1) (1 ml/100 mg of resin) at room temperature for 3

h. The resin was filtered off and crude products were precipitated with cold Et₂O. The resulting solid was centrifuged and washed twice with ether, and then lyophilized.

Peptide purification and characterization. Peptides were purified by MPLC using SNAP 12 g KP-C18-HS cartridges in an ISOLERA ONE (BIOTAGE). A gradient of CH₃CN:H₂O (0.05% TFA) from 0:100 to 30:70 over 60 min, as mobile phase, and a flow of 5 mL/min were used. Some peptides were purified by semipreparative RP-HPLC-MS (Waters 2545) coupled to a mass spectrometer 3100 detector, using a SUNFIRE™ column C18 (5 μ, 10 x 150 mm) and an 8 mL/min flow with a gradient of CH₃CN (0.1% HCO₂H) [Solvent A]:H₂O (0.1% HCO₂H) [Solvent B] as mobile phase. The purity of peptides was analyzed using an analytical HPLC Waters (model 2690) with a SUNFIRE™ column C₁₈ (3.5 μ, 4.6 x 50 mm, 1 mL/min) with a 5 min gradient of CH₃CN (0.005% HCO₂H) [Solvent A]:H₂O (0.005% HCO₂H) [Solvent B] as mobile phase, or on Agilent apparatus (model 1120 Compact LC) equipped with an Eclipse Plus column C₁₈ (4.6 x 150 mm) at 1.5 mL/min flow, and passing a 5 to 80 gradient of CH₃CN [Solvent A]:H₂O (0.05% TFA) [Solvent B] as mobile phase, over 20 min. Characterization of the products was performed by simple ESI-MS (Waters, Micromass ZQ 2000) and HRMS (EI+, Agilent 6520 Accurate-Mass Q-TOF LC/MS equipment).

Ac-FEKRRNPAAGLIQSAWRFYATN(2-(2-(2-(2-azidoethoxy)ethoxy)ethoxy)ethyl)-NH₂ (2). Resin-bound peptide (500 mg, 0.17 mmol) **1**, incorporating Asp(OAll) at C-terminal, was synthesized using general coupling procedure described above. After acetylation and OAll protecting group removal, a solution of 11-azido-3,6,9-trioxaundecen-1-amine (67.46 μL, 0.34 mmol), HCTU (141 mg, 0.34 mmol), DIEA (59 μL, 0.34 mmol) in 5 mL anhydrous DMF was added to the resin. After 2 h at room temperature, the excess of reagents were drained and the resin washed with DMF/DCM/DMF/DCM (5 x 0.5 min) and checked by the Kaiser test. The peptide was cleaved as indicated above, and purified by MPLC to lead to 21 mg (5% total yield) of a white lyophilized solid with a purity of 99%. HPLC (Eclipse Plus column C₁₈): t_R = 10.25 min. ESI-MS: [M + 3H]³⁺ = 947.48. HRMS (EI+) m/z 2837.4873 ([M]⁺ C₁₂₈H₁₉₆N₄₀O₃₄, requires 2837.4838).

Alkyne-PEG Peptides 5 and 6. Resin-bound peptides **3** and **4** (500 mg, 0.17 mmol), incorporating Fmoc-Lys(Alloc) at N-terminal, were synthesized using the general coupling procedure, followed by acetylation and Alloc protecting group removal, as described above. A solution of 2-[2-(Fmoc-amino)ethoxy]ethoxy] acetic acid (131 mg, 0.34 mmol), HCTU (141 mg, 0.34 mmol), DIEA (59 μL, 0.34 mmol) in 5 mL of anhydrous DMF was then added, and the reaction continued at room temperature for 2 h. After complete coupling, the resin was washed, drained and checked by the Kaiser test. The resin-bounded peptide was treated with 20% piperidine in DMF, to remove the Fmoc group on the amino-PEG chain, washed rigorously with DMF/DCM/DMF/DCM (5 x 0.5 min) and treated with a solution of 4-pentynoic acid (34 mg, 0.34 mmol) in anhydrous DMF, HCTU (141 mg, 0.34 mmol) and DIEA (59

μL , 0.34 mmol) for 2 h at room temperature. The resin was washed with DMF/DCM/DMF/DCM (5 x 0.5 min), drained and checked until the ninhydrin test was negative. The corresponding peptide was cleaved following the general procedure described above.

Ac-K[2-(2-(Pent-4-ynamido)ethoxy)ethoxy]acetyl]VSIRAVCVMRFLVSKRKF-NH₂ (5). Purification by MPLC led to 44 mg (9% yield) of a white lyophilized solid with a purity of 98%. HPLC-MS (SUNFIRETM column C₁₈): $t_{\text{R}} = 2.75$ min with a 5 min gradient from 10 to 100 of CH₃CN (0.08% HCO₂H):H₂O (0.01% HCO₂H) as mobile phase. ESI-MS: $[\text{M} + 5\text{H}]^{5+} = 507.90$. HRMS (EI+) m/z 2532.4567 ($[\text{M}]^+\text{C}_{116}\text{H}_{197}\text{N}_{33}\text{O}_{26}\text{S}_2$, requires 2532.4549).

Ac-K[2-(2-(Pent-4-ynamido)ethoxy)ethoxy]acetyl]VSIRAVRVLRLFLVSKRKF-NH₂ (6). Purification by semipreparative RP-HPLC-MS with a gradient 2:98 to 40:60 (A:B) in 15 min. Yield (8 mg, 1%), white lyophilized solid with a purity of 99%. HPLC (SUNFIRETM column C₁₈): $t_{\text{R}} = 2.72$ min in 5 a min gradient 10:90 to 100:0 of (A:B) as mobile phase. ESI-MS: $[\text{M} + 3\text{H}]^{3+} = 862.56$. HRMS (EI+) m/z 2582.6165 ($[\text{M}]^+\text{C}_{121}\text{H}_{208}\text{N}_{36}\text{O}_{26}$, requires 2582.6139).

Synthesis of peptide conjugates 7 and 8 by Click chemistry.

General procedure for the Click reaction of alkyne- and azide-PEG-peptide derivatives. Alkyne peptides **5** or **6** (4.22 μmol) were dissolved in H₂O/^tBuOH (2:1, 10 mL), and azide peptide **2** (4.22 μmol), CuSO₄·5H₂O (11 mg, 42.2 μmol), and sodium ascorbate (13 mg, 63.3 μmol) were added. The resulting mixtures were stirred at room temperature overnight, and QuadraSil[®]MP (85 μmol) was added, stirred for 10 min and filtered. The solutions were then concentrated and lyophilized. Crude products were purified by semipreparative RP-HPLC-MS to yield the corresponding 1,4-disubstituted 1,2,3-triazolyl-PEG-peptides.

1-[Ac-FEKRRNPAAGLIQSAWRFYATN(2-(2-(2-ethoxy)ethoxy)ethoxy)ethyl)-NH₂]-4-[Ac-K(2-(2-Propanamide)ethoxy)ethoxy]acetyl]VSIRAVCVMRFLVSKRKF-NH₂]-1,2,3-triazole (7). Purified with a gradient from 2:98 to 30:70 (A:B) in 30 min. Yield (2 mg, 8%), white lyophilized solid with a purity of 98%. HPLC (Eclipse Plus column C₁₈): $t_{\text{R}} = 9.86$ min. ESI-MS: $[\text{M} + 5\text{H}]^{5+} = 1076.13$, $[\text{M} + 6\text{H}]^{6+} = 899.23$, $[\text{M} + 7\text{H}]^{7+} = 768.81$, $[\text{M} + 8\text{H}]^{8+} = 672.84$. HRMS (EI+) m/z 5369.9375 ($[\text{M}]^+\text{C}_{244}\text{H}_{393}\text{N}_{73}\text{O}_{60}\text{S}_2$, requires 5369.9387).

1-[Ac-FEKRRNPAAGLIQSAWRFYATN(2-(2-(2-ethoxy)ethoxy)ethoxy)ethyl)-NH₂]-4-[Ac-K(2-(2-Propanamide)ethoxy)ethoxy]acetyl]VSIRAVRVLRLFLVSKRKF-NH₂]-1,2,3-triazole (8). Purified with a gradient from 2:98 to 40:60 (A:B) in 15 min. Yield (1.4 mg, 6%), white lyophilized solid with a purity of 99% (total yield). HPLC (Eclipse Plus column C₁₈): $t_{\text{R}} = 9.84$ min. ESI-MS: $[\text{M} + 7\text{H}]^{7+} = 773.85$. $[\text{M} + 8\text{H}]^{8+} = 677.58$. $[\text{M} + 9\text{H}]^{9+} = 602.08$. $[\text{M} + 10\text{H}]^{10+} = 541.91$. HRMS (EI+) m/z 5419.0839 ($[\text{M}]^+\text{C}_{249}\text{H}_{404}\text{N}_{76}\text{O}_{60}$ requires 5419.0898).

Proteins. Recombinant rat brain calmodulin (CaM) was produced in E.coli strain BL21-DE3 and purified as described.⁹ Dispersion of the samples was evaluated by dynamic light scattering (DLS) using a Zetasizer Nano instrument (Malvern Instruments Ltd.) in order to exclude the presence of aggregates.

Fluorometry. Fluorescent dansylated CaM (D-CaM, 5-(dimethylamino)naphthalene-1-sulfonyl-calmodulin) was prepared using recombinant CaM and dansyl chloride as described.³³ CaM with a T to C mutation at threonine 34 or 110 and labeled with 5-(((2-iodoacetyl)amino)ethyl)-amino)naphthalene-1-sulfonic acid (1,5-IAEDANS) to give A34-CaM and A110-CaM respectively, were kindly provided by Katalin Török (Division of Basic Medical Sciences, St George's University of London, London, UK). Prior to the experiments, D-CaM and AEDANS-CaMs were dialyzed against 2 L of buffer containing 25 mM Tris-HCl (pH 7.4), 120 mM KCl, 5 mM NaCl, 2 mM MgCl₂ for 48 h, changing the buffer every 12 h. Steady-state fluorescence measurements were performed with an Aminco Bowman series 2 (SLM Aminco) fluorescence spectrophotometer in a final volume of 100 µl (using quartz cuvette) at 25 °C. The excitation wavelength was 340 nm and emissions were recorded from 400 to 660 nm. Slit widths were set at 4 nm for excitation and 4 nm for emission. Peptides (0-800 nM) from a concentrated stock solution were incubated with D-CaM or the indicated AEDANS-CaM in 25 mM Tris-HCl (pH 7.4), 120 mM KCl, 5 mM NaCl, 2 mM MgCl₂, 10 mM EGTA or in the same buffer in the presence of calcium excess (by adding 9.63 mM Ca²⁺ to give a concentration of 3.9 µM free Ca²⁺). Free Ca²⁺ concentration was determined using Fura-2 (Invitrogen) following the manufacturer's instructions. The concentration of D-CaM or AEDANS-CaMs (12.5-400 nM) was varied, and concentration-response curves were generated for fluorescence enhancement vs [ligand] to each D-CaM (or AEDANS-CaM) concentration. The parameters of the Hill equation (Fluorescence increase = $A \times [\text{ligand}]^h / EC_{50} + [\text{ligand}]^h$; where A is the maximal fluorescence increase and h is the Hill coefficient) were fitted to the data by curvilinear regression, enabling the apparent affinity (EC₅₀ or concentration that gives half-maximal change in fluorescence emission intensity) and Hill coefficient to be determined. EC₅₀ values were plotted against the concentration of D-CaM (or AEDANS-CaM) to estimate the true affinities from the y axis intercept. Data are shown as average of three or more independent experiments. For all measurements, it has been subtracted the small contribution of the peptide signal because they emit at 425 nm after being excited, in solution, at 340 nm.

ACKNOWLEDGMENTS

This research was supported by Consolider-Ingenio CSD2008-00005 (SICI, to AV, RGM, and OM), BFU2012-39092-C02-02 (to RGM) and BFU2012-39883 (to AV). M.A.B. thanks the CSIC for a JAE-doc contract from the Program «Junta para la Ampliación de Estudios», co-financed by the ESF. A.A. was supported by Fundación Biofísica Bizkaia and by Universidad del País Vasco (UPV/EHU) postdoc-

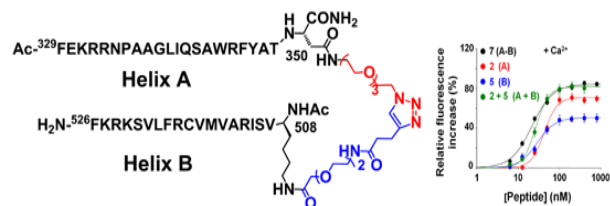
toral fellowship. C.M. was co-funded by Spanish Ministry of Economy and Competitiveness (PTA2012) and by Fundación Biofísica Bizkaia.

REFERENCES

1. M. V. Soldovieri, F. Miceli and M. Tagliatela, *Physiology* 2011, **26**, 365.
2. Y. Haitin and B. Attali, *J. Physiol* 2008, **3**, 1803.
3. E. Yus-Nájera, I. Santana-Castro and A. Villarroel, *J. Biol. Chem.* 2002, **277**, 28545.
4. A. Etxeberria, P. Aivar, J. A. Rodriguez-Alfaro, A. Alaimo, P. Villace, J. C. Gomez-Posada, P. Areso and A. Villarroel, *FASEB J.* 2008, **22**, 1135.
5. N. Gamper and M. S. Shapiro, *J. Gen. Physiol.* 2003, **122**, 17.
6. A. A., Selyanko and D. A. Brown, *Neuron* 1996, **16**, 151.
7. G. Bellini, F. Miceli, M. V. Soldovieri, G. E. Miraglia, G. Coppola and M. Tagliatela, *GeneReviews* 2010. <http://www.ncbi.nlm.nih.gov/books/NBK32534/>.
8. S. Weckhuysen, S. Mandelstam, A. Suls, D. Audenaert, T. Deconinck, L.R. Claes, L. Deprez, K. Smets, D. Hristova, I. Yordanova, A. Jordanova, B. Ceulemans, A. Jansen, D. Hasaerts, F. Roelens, L. Lagae, S. Yendle, T. Stanley, S. E. Heron, J. C. Mulley, S. F. Berkovic, I. E. Scheffer and D. J. Peter, *Ann. Neurol.* 2012, **71**, 15.
9. A. Alaimo, J. C. Gómez-Posada, P. Aivar, A. Etxeberria, J. A. Rodriguez-Alfaro, P. Areso and A. Villarroel, *J. Biol. Chem.* 2009, **284**, 20668.
10. F. S. Choveau and M. S. Shapiro, *Frontiers Physiol.* 2012, **3**, 1.
11. K. Mruk, S. M. D. Shandilya, R. O. Blaustein, C. A. Schiffer and W. R. Kobertz, *Proc. Natl. Acad. Sci. USA* 2012, **109**, 13579.
12. Q. Xu, A. Chang, A. Tolia and D. L. Minor, Jr., *J. Mol. Biol.* 2013, **425**, 378.
13. A. Alaimo, A. Alberdi, C. Gomis-Perez, J. Fernandez-Orth, G. Bernardo-Seisedos, C. Malo, O. Millet, P. Areso and A. Villarroel, *PLoS ONE* 2014, **9**, e86711.
14. A. Alaimo, A. Alberdi, C. Gomis-Perez, J. Fernandez-Orth, J. C. Gomez-Posada, P. Areso and A. Villarroel, *J. Cell Sci.* 2013, **126**, 244.
15. M. A. Schumacher, A. F., H. P. Rivard, Bachinger and J. P. Adelman, *Nature* 2001, **410**, 1120.
16. P. Aivar, J. Fernandez-Orth, C. Gomis-Perez, A. Alberdi, A. Alaimo, M. S. Rodriguez, T. Giraldez, P. Miranda, P. Areso and A. Villarroel, *PLoS ONE* 2012, **7**, e47263.
17. P. Thirumurugan, D. Matosiuk and K. Jozwiak, *Chem. Rev.* 2013, **113**, 4905.
18. M. Bähler and A. Rhoads, *FEBS Lett.* 2002, **513**, 107.

19. F. J. Dekker, N. J. de Mol, J. van Ameijde, M. J. E. Fischer, R. Ruijtenbeek, F. A. M., Redegeld and R. M. J. Liskamp, *ChemBioChem* 2002, **3**, 238.
20. M. Neshar, Y. Vachutinsky, G. Fridkin, Y. Schwartz, K. Sasson, M. Fridkin, Y. Shechter and D. Lichtstein, *Bioconjugate Chem.* 2008, **19**, 342.
21. M. Danial, T. H. H. van Dulmen, J. Aleksandrowicz, A. J. G. Pötgens and H.-A. Klok, *Bioconjugate Chem.* 2012, **23**, 1648.
22. A. Jain and H. S. Ashbaugh, *Biomacromolecules* 2011, **12**, 2729.
23. E. Hamed, T. Xu and S. Keten, *Biomacromolecules* 2013, **14**, 4053.
24. A. I. Fernández-Llamazares, J., F. Adan, Mitjans, J. Spengler and F. Albericio, *Bioconjugate Chem.* 2014, **25**, 11.
25. G. E. Mulder, J. A. W. Kruijtzter and R. M. J. Liskamp, *Chem. Commun.* 2012, **48**, 10007.
26. A. I. Fernández-Llamazares, J. García, J. Adan, D. Meunier, F. Mitjans, J. Spengler and F. Albericio, *Org. Lett.* 2013, **15**, 4572.
27. J. Xiao and T. J. Tolbert, *Bioorg. Med. Chem. Lett.* 2013, **23**, 6046.
28. M. Van Dirk, C. F. van Nostrum, W. E. Hennink, D. T. S. Rijkers and R. M. J. Liskamp, *Biomacromolecules* 2010, **11**, 1608.
29. J. C. Slootweg, S. van der Wal, H. C. Quarles van Ufford, E., Breukink, R. M. J. Liskamp and D. T. S. Rijkers, *Bioconjugate Chem.* 2013, **24**, 2058.
30. S. A. Kates and F. Albericio, *Solid-Phase Synthesis. A practical guide.* Ed. Marcel Dekker INC., New York, 2000.
31. E. Valeur and M. Bradley, *Chem. Soc. Rev.* 2009, **38**, 606.
32. J. Xiao and T. J. Tolbert, *Org. Lett.* 2006, **18**, 4144.
33. A. Alaimo, C. Malo, K., O. Aloria, Millet, P. Areso and A. Villarroel, *Methods Mol. Biol.* 2013, **998**, 217.

TOC



Small bis-conjugates HelixA³²⁹⁻³⁵⁰-PEG-triazole-PEG-HelixB⁵⁰⁸⁻⁵²⁶ (41 residues), prepared through click chemistry of PEGylated peptide derivatives, bind to CaM with nanomolar affinity, behaving as mimics of the Kv7.2 native fragment (239 residues).